

# Pencil slip in beta-tin single crystals

S. N. G. CHU, J. C. M. LI

*Materials Science Program, Department of Mechanical and Aerospace Sciences, University of Rochester, Rochester, New York 14627, USA*

Pencil slip was observed when a punch was pressed over the (0 0 1) surface of a  $\beta$ -tin single crystal. A bulge of similar size and shape as the punch appeared at the opposite surface directly across the thickness of the crystal. Slip line observations inside the sample showed slip activity confined to a cylindrical shell whose inner diameter was the same as the punch and whose axis was parallel to the [0 0 1] direction. The thickness of the slip shell increased with the punching stress and with the ratio between punch diameter and sample thickness. The effects of punching stress on the entering velocity of the punch and on the exiting velocity of the bulge were studied and the results compared with those of impression creep reported previously. The situation in which the bulge was not allowed to form was also studied.

## 1. Introduction

Pencil slip or prismatic punching is a rare slip phenomenon. It occurs only in crystals with a unique crystallographic slip direction and several slip planes which can form a closed prism whose axis is parallel to the slip direction. When a concentrated stress, such as that due to a punch, is applied to the crystal surface in the slip direction, the material will glide along the prism planes as if a prism or cylinder of material is pushed out of the solid.

The phenomenon was first discovered by Taricco [1], as mentioned by Nabarro [2], in a PbS single crystal. When a blunt indenter was tapped sharply on the (0 0 1) cleavage face, a square pyramid rose on the opposite (0 0 1) face with the edges of the base of the pyramid parallel to the [0 0 1] and [0 1 0] directions. Mügge [3] (see also [2]) observed the same phenomenon in tetragonal phosgenite and showed that the mechanisms for both PbS and phosgenite were caused by crystallographic glide. Similar phenomena existed in bcc iron [4], mercury [5] and silver chloride [6] by observing that these crystals sometimes had corrugated slip surfaces made up of strips of slip planes sharing a common slip direction. On a macroscopic scale the apparent slip surface may not be a crystallographic plane. The slip surface may be determined by maximum

resolved shear stresses. Taylor [4] was the first to model pencil slip by a bundle of rods slipped along their length. Later Nye [6] called it pencil slip. In the same year Smakula and Klein [7] demonstrated that the strain produced by a blunt punch on (1 0 0), (1 1 0), or (1 1 1) faces of a bcc thallium halide single crystal can be transmitted along cubic directions to the opposite cubic faces where truncated square pyramids appeared with edges parallel to the  $\langle 1 1 0 \rangle$  directions. Seitz [8] named this phenomenon prismatic punching and proposed prismatic dislocations of  $\langle 1 0 0 \rangle$  Burgers vectors gliding along the prism formed by  $\{0 1 1\}$  slip planes as the mechanism for transmitting the strain.

In this work, complete pencil slip caused by a cylindrical punch was observed for the first time in a  $\beta$ -tin single crystal. The crystal structure is body-centered tetragonal. Pencil slip was found to occur in the [0 0 1] direction surrounded by (1 1 0) and  $(\bar{1} 1 0)$  planes. The effects of punch size, punching stress and crystal thickness on the shape and velocity of the cylinder (or bulge) slipping out of the opposite surface were studied. Possible slip systems involved in the process are discussed.

## 2. Experimental details

A single crystal ingot of  $\beta$ -tin was grown by

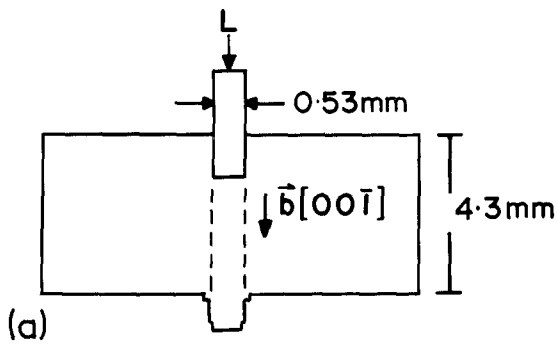
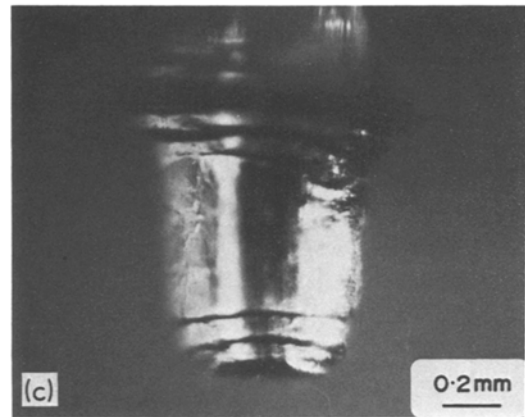
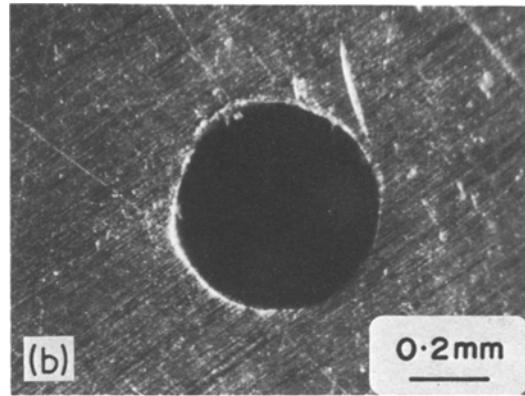


Figure 1 Typical pencil slip behaviour in a  $\beta$ -tin single crystal: (a) the general arrangement; (b) the impression made on the top surface; (c) the bulge slipped out of the bottom surface.



vacuum zone melting. Granules of 99.9% purity were melted and zone refined prior to crystal growth. The single crystal ingot was believed to be of better than 99.99% purity. Crystal orientations were determined by the X-ray back-reflection method. Slabs parallel to the (001) plane were acid sawn from the single crystal ingot. The surfaces were further polished on an acid planer. Five sample thicknesses of 3.4 mm, 4.1 mm, 4.3 mm, 6.4 mm, and 11.5 mm were used.

To demonstrate the pencil slip in  $\beta$ -tin, two different kinds of punches were used. One was cylindrical in shape and the other was a punch of the letter "Y". During the test, the bottom of the sample can be supported either by a hard surface (closed-end) so as to prevent the bulge from

developing or by the use of a hole to allow the bulge to form (open-end).

To reveal slip activities inside the crystal, a technique involving the use of two half crystals

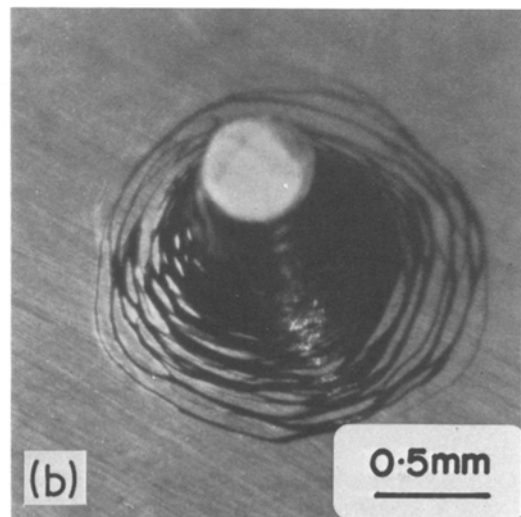
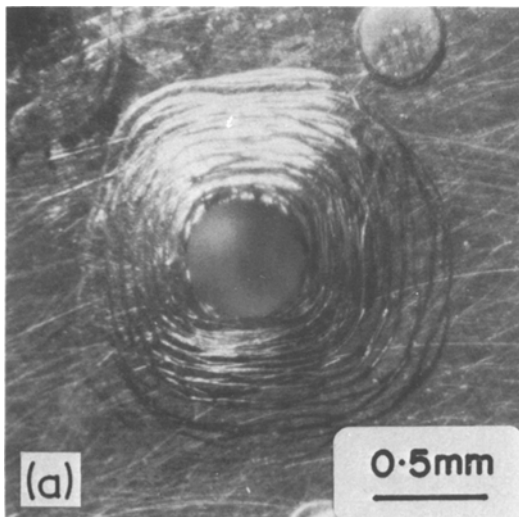
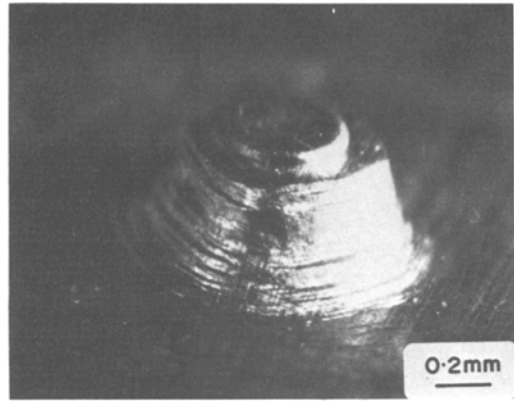
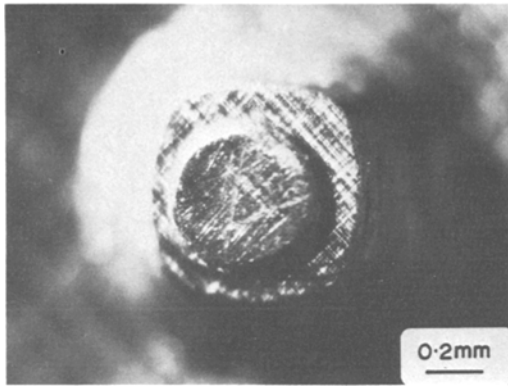


Figure 2 Gradual change of cross-section from circular to square shapes: (a) inverted pyramidal hole on the top surface; (b) pyramidal bulge on the bottom surface.



*Figure 3* Abrupt change of the cross section of bulge due to a sudden change of punching stress.

cut from a single crystal and clamped together before punching was used. The details are to be described later.

Quantitative measurements of entering velocity of the punch (punching velocity) and the exiting velocity of the bulge at the bottom of the crystal were made as a function of punching stress and the size of the punch. These experiments were done in an impression creep apparatus described before by Chu and Li [9] with a modification in the crystal support in the case of open-end to allow the material to slip out of the bottom surface of the crystal slab and at the same time to

record the height of the bulge as a function of time. After the test the bulge was polished off on emery paper so that the crystal could be used again by punching at another location. All the tests, except the one with the letter punch, were done in air at a temperature of  $29.7 \pm 0.4^\circ \text{C}$ . The test using the letter punch was conducted at room temperature in air by placing the single crystal slab on a thin sheet of rubber or a thick paper towel and tapping gently with the letter punch on the top surface of the crystal.

To observe delayed pencil slip, an impression was made on the top surface over a rigid support

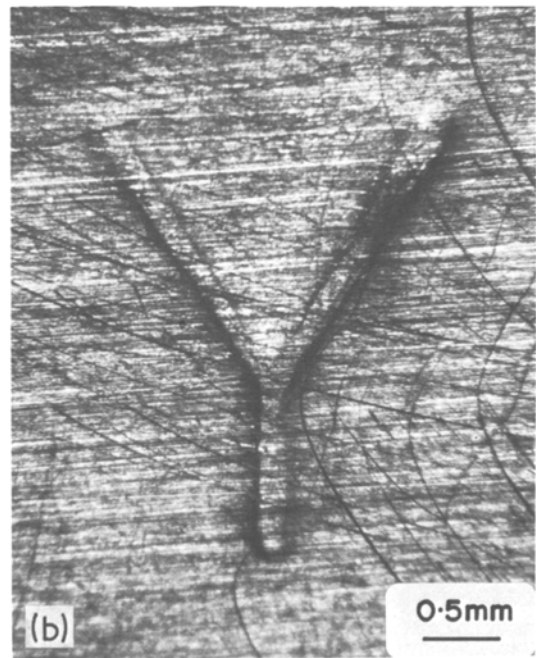
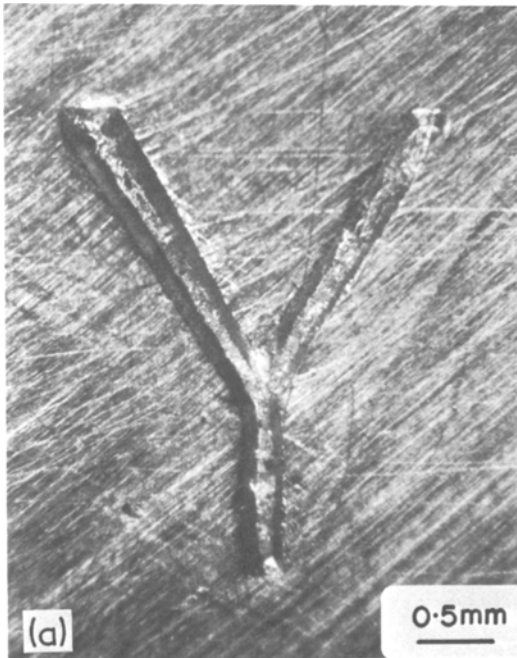


*Figure 4* Pencil slip caused by a letter punch: (a) the Y-shaped impression ( $< 0.5$  mm deep) on the top surface; (b) the Y-shaped bulge on the bottom surface (sample thickness = 4.3 mm).

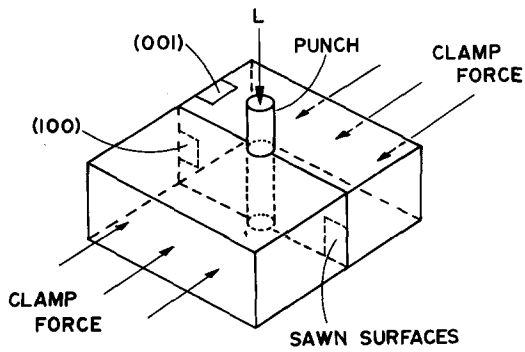


Figure 5 Schematic diagram for a pencil slip test on clamped half-crystals cut from a single crystal to reveal internal slip activities.

so that no bulge was formed. Then the dented sample was transferred to a support with a hole without the load and the delayed bulging was recorded.

### 3. Experimental results

#### 3.1. General behaviour

When a flat-end cylindrical punch was pushed into the (001) surface of a  $\beta$ -tin single crystal in the  $[00\bar{1}]$  direction, a bulge of the shape of a cylinder was formed at the bottom surface as shown in Fig. 1. The upper picture shows the hole made by the cylindrical punch on the top (001) surface and the lower picture shows the cylinder (bulge) slipped out of the bottom (00 $\bar{1}$ ) surface of the crystal slab. Except near the end of the cylinder where the cross section has the same size and shape as the punch, the cross section gradually increases in size and changes from circular to square shapes whose edges are parallel to  $[110]$  and  $[1\bar{1}0]$  directions. Such gradual change is shown more clearly in Fig. 2. The lines are the slip steps formed over the pyramidal surface. The

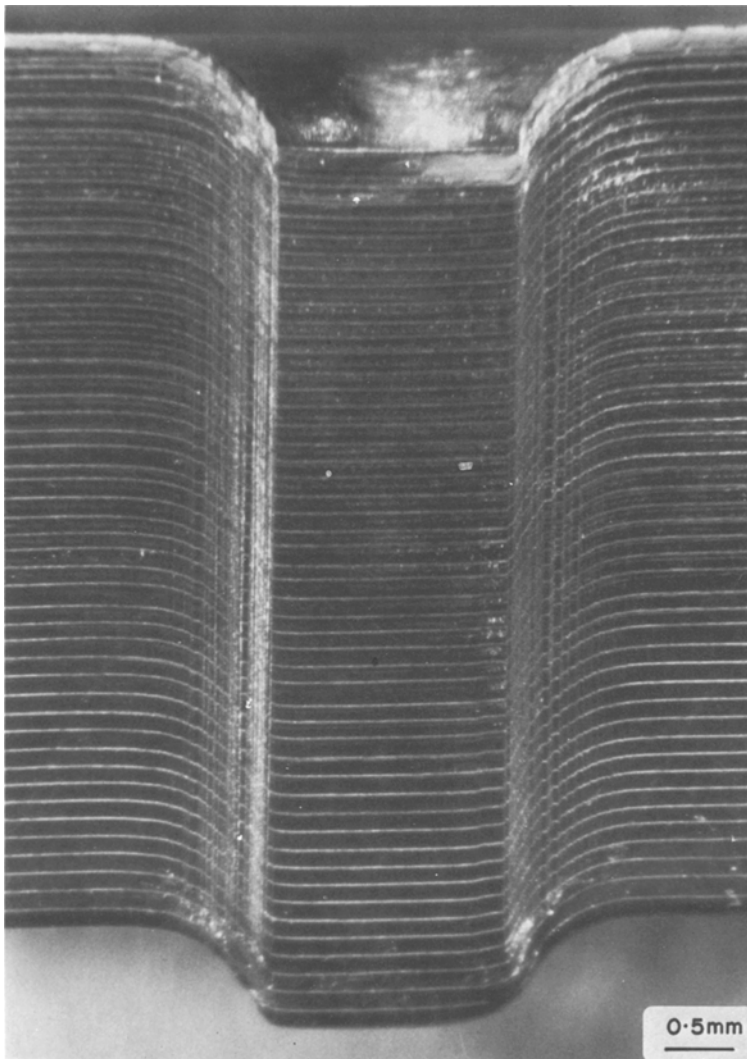


Figure 6 Slip lines and the distortion of scratches on the sawn surface for the open-end case.

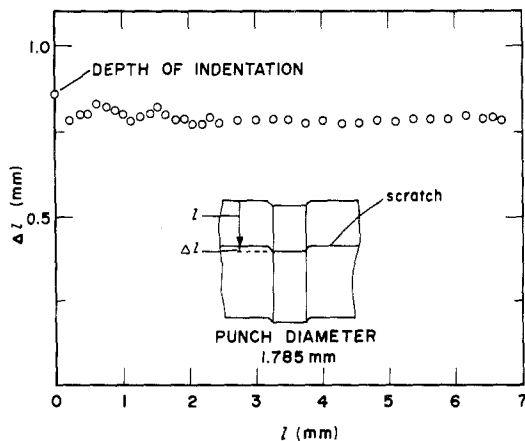


Figure 7 Displacement of scratches measured along the thickness direction of the sample for the open-end case.

degree of gradual change in cross section depends on the punching stress, the diameter of the punch and the thickness of the sample. For very low stress, the bulge can have the same size and shape as the punch with very little change in the cross section. Upon increasing the stress, the cross section increases in size and changes into a square shape. This change is accompanied by a similar change in the top surface as shown in Fig. 2. Such changes are more pronounced for a large punch diameter or for a thin crystal (such as a ratio of 0.18 between the two quantities). Upon a large increase in stress, both the size and the shape can change suddenly as shown in Fig. 3.

The height of the cylinder (bulge) is always less than the depth of the hole on the top surface. Similarly the exiting speed of the bulge is always less than the entering speed of the punch. Details will be reported later.

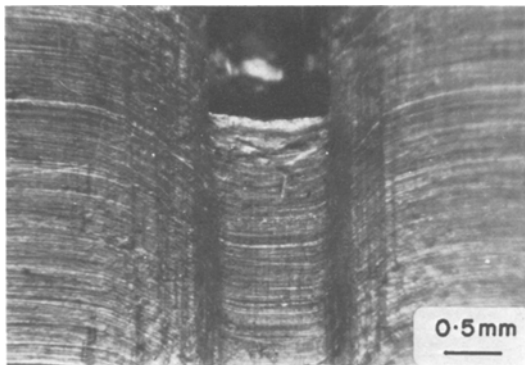


Figure 8 Slip activities in a thicker cylindrical shell produced in the open-end case in which the punch diameter to sample thickness ratio, ( $d/T$ ), was 0.33 instead of 0.28 as in Fig. 5.

To demonstrate pencil slip for a punch of more complicated geometry, a punch of the letter "Y" was used. The thickness of the sample was 4.3 mm and the size of the "Y" was about 2.5 mm  $\times$  3.4 mm. The impression made on the top surface is shown in Fig. 4a and was about 0.5 mm deep. A letter "Y" of exactly the same size appeared on the bottom surface as shown in Fig. 4b.

### 3.2. Slip lines appeared on the sawn surfaces

To reveal slip activities inside the sample, a thick slab was cut into two halves along (1 0 0) before the test. This was achieved by an acid saw and the sawn surfaces were subjected to fine mechanical polishing with Isocut fluid, by Buehler Ltd, as lubricant. Parallel scratches of equal spacing (about 100  $\mu$ m) were introduced perpendicular to [0 0 1] on each polished sawn surface. This was done with the help of a measuring microscope modified for such a purpose. The two halves of the sample were clamped together by pressing the sawn surfaces facing each other through a layer of lubricant. The clamped sample was then loaded by a punch along the boundary as shown in Fig. 5. After the test, the sawn surfaces were examined in an optical microscope.

#### 3.2.1. Open-end case

The slip lines and their distortion of the scratches are shown in Fig. 6 for the case in which the sample support had a hole to allow the bulge to form at the bottom surface. The displacement of the scratches is plotted in Fig. 7 as a function of the depth,  $l$ , measured from the undeformed top surface. It is seen that the cylinder whose diameter is the same as that of the punch slipped as a rigid piece relative to the rest of the sample. Except for the slip band region of the shape of a cylindrical shell surrounding the cylinder (pencil), the rest of the material was not deformed at all. These observations seem to confirm to what Taylor [4] proposed some fifty years ago.

The punch diameter to sample thickness ratio, ( $d/T$ ) was 0.28 for the case shown in Fig. 6. The case of a larger ( $d/T$ ) ratio (0.33) is shown in Fig. 8 where a thicker cylindrical shell was formed. The depth of the impression is usually larger than the height of the bulge, but they approach each other for low stresses, large punches, and/or thin samples.

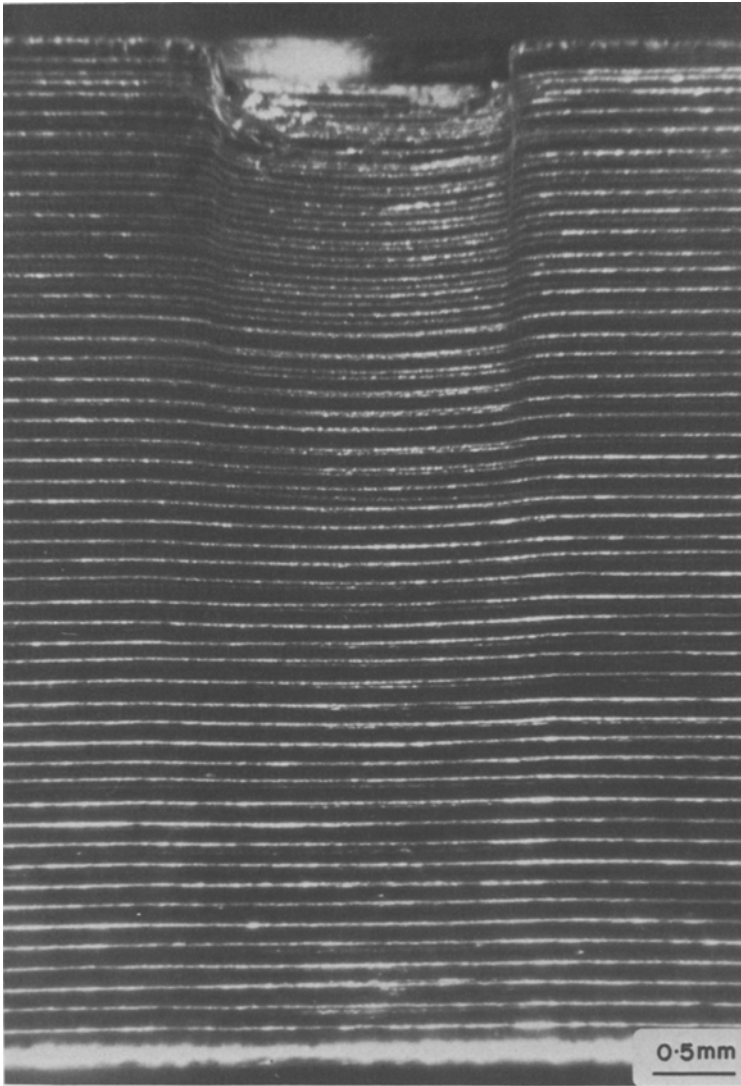


Figure 9 Slip lines and the distortion of scratches on the sawn surface for the closed-end case.

### 3.2.2. Closed-end case

Fig. 9 shows the slip lines and the distortion of the scratches for the case in which the sample support was rigid so that the bulge was not permitted to form. It is seen that the displacement of the scratches is no longer uniform. As shown in Fig. 9 the displacement is large near the top surface and gradually decreases to zero near the bottom surface of the specimen. The slope of the curve or the gradient of the displacement (plastic strain) is large near the top surface and gradually decreases to a small value at the bottom surface of the specimen. The displacement gradient can be taken as the linear density of dislocation loops (prismatic interstitial loops whose radii are the same as the radius of the punch) so that Fig. 10

should be consistent with a pile-up of circular dislocations. However, theoretical calculations for the equilibrium of a large number of circular dislocations are not available at present for a quantitative comparison. Nevertheless, the distribution of displacements resembles that of a single pile-up of straight dislocations as shown in Fig. 11. The curve was obtained by integration of  $[(l_0 - l)/l]^{1/2}$  with respect to  $l$  from  $l$  to  $l_0$  [10, 11] with  $l_0$  being the length of the pile-up. The result is proportional to the displacement  $\Delta l$  at  $l$ . The displacement at  $l = 0$  is designated  $\Delta l^*$ . It is seen that the curve is similar to that of Fig. 10.

An attempt to study the effect of annealing on the recovery of the displacement of scratches

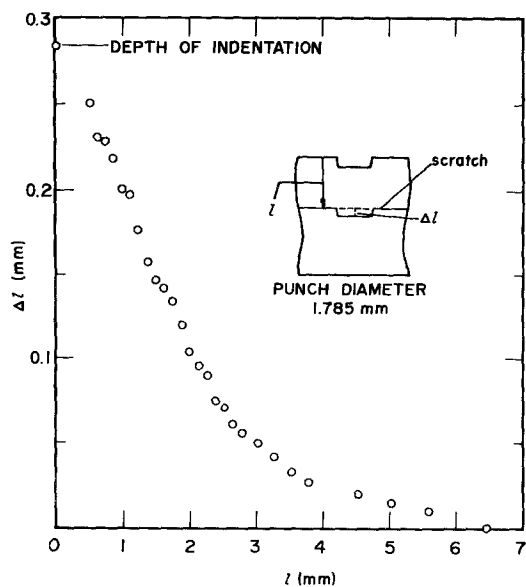


Figure 10 Displacement of scratches measured along the thickness direction of the sample for the closed-end case.

was not successful. The region underneath the punch recrystallized instead.

### 3.3. Effect of punching stress on impressing velocity

As expected, the punching velocity or the entering velocity of the punch varies with the punching stress following a power law as shown in Fig. 12 for both the open-end and the closed-end cases. The exponent is usually 4, the same as that

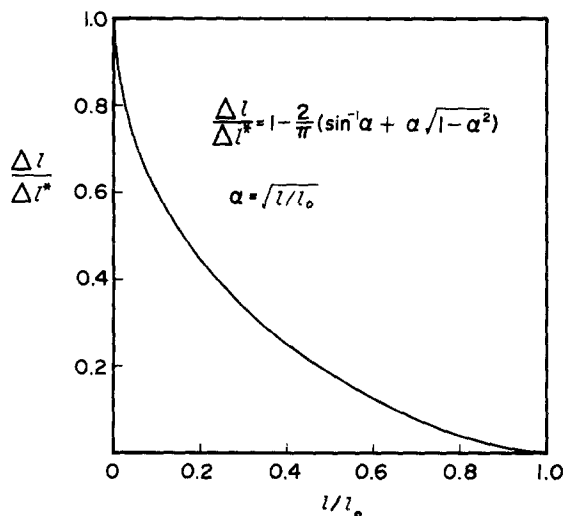


Figure 11 Displacement distribution due to a single pile-up of straight dislocations.

obtained before [9] except in one case where the punching stress was high and the punch was approaching the bottom surface to cause unstable deformation. In general the punching velocity is higher in the open-end case than in the closed-end case under otherwise identical conditions.

### 3.4. The effect of diameter to thickness ratio

The effect of specimen thickness is obviously important especially in the open-end case. The power law of exponent 4 is for large thicknesses or small punch diameter-to-thickness ratios as shown in Fig. 12. Small thicknesses or large diameter-to-thickness ratios tend to exaggerate the effect of the stress dependence on punching velocity, see Fig. 13. Starting with a thick specimen, the punching velocity–punching stress relation obeyed a power law of exponent 4 until the penetration of the punch was so deep that the diameter/remaining-thickness ratio reached about 0.36. For deeper penetration the exponent began to increase. This is illustrated in Fig. 13.

### 3.5. The exiting velocity of the bulge

When the bulging velocity at the bottom surface (open-end case) was measured simultaneously with the entering velocity of the punch (the punching velocity) at the top surface, the former was always smaller than the latter with a ratio of about 0.4. However, their dependences on punching stress are similar as seen in Fig. 14. Since the data were obtained from the same hole for the same sample thickness, the stress exponent increased after a critical  $d/t$  ratio as the punch penetrated into the sample. When this happens, the punching velocity became more sensitive to the punching stress as seen in Fig. 14.

### 3.6. Delayed bulging

Delayed bulging was observed in the closed-end case after the impression was made, the load was removed and the bottom surface was left free. The bulging velocity was fast in the beginning and gradually decreased to zero.

However if the temperature was 200°C no delayed bulging was observed. Instead, recrystallization was found to take place.

## 4. Discussion

The crystal structure of  $\beta$ -tin is body-centred tetragonal with a  $c/a$  ratio of 0.5457. From slip

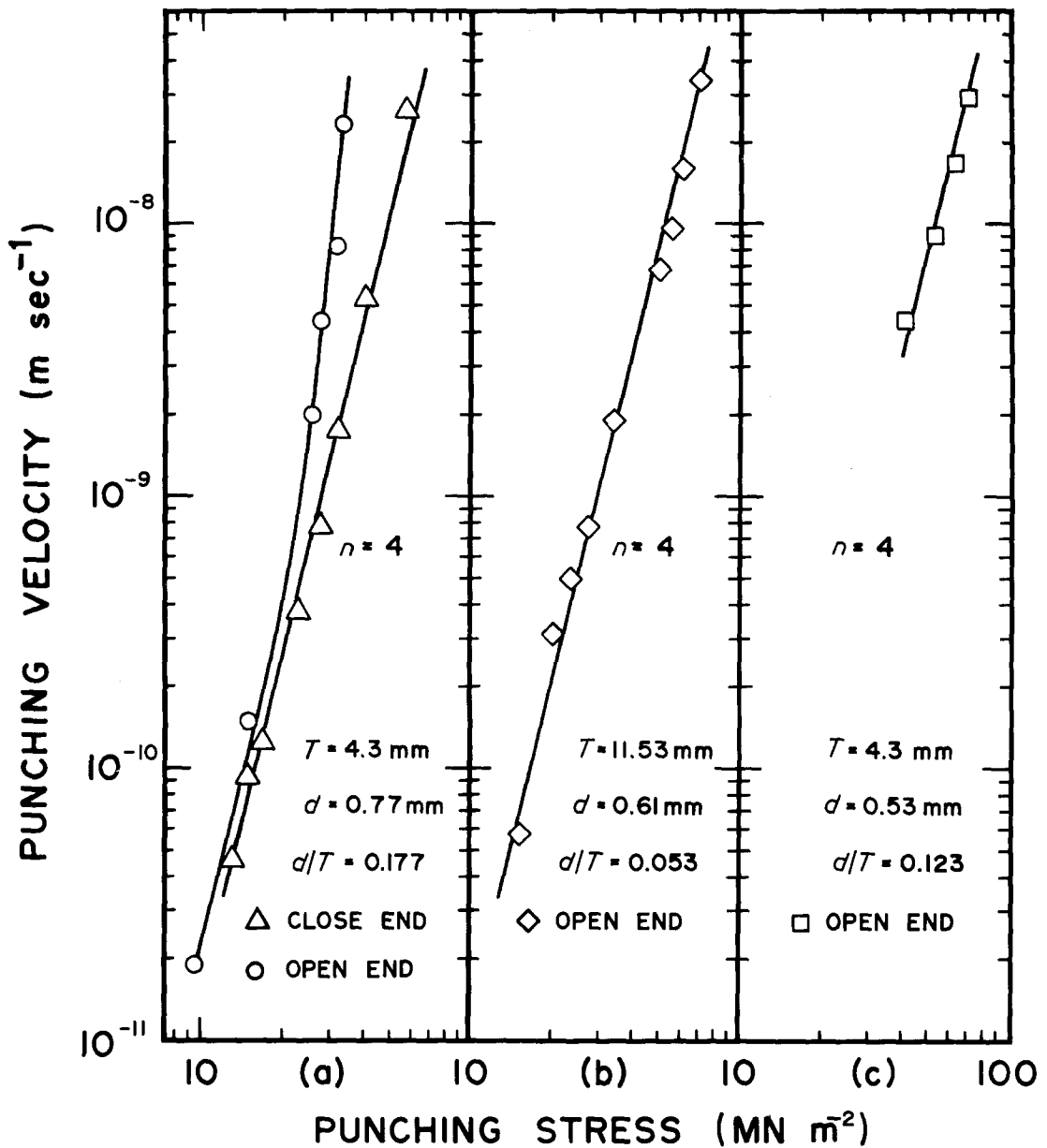


Figure 12 Stress dependence of punching velocity for both the open-end and the closed-end cases.

line observations [9] on the (001) surface after [001] punching, the possible slip systems are (110) [001] and (110) [ $\bar{1}11$ ] types. However, from internal slip line observations of Figs. 6 and 9, the major slip system is probably (110) [001] and (1 $\bar{1}0$ ) [001]. Such slip systems are consistent with the gradual change of the cross section of the bulge from circular to square shapes.

Since the inside cylinder seems not at all deformed, as shown in Fig. 6 in the open-end case,

the slip activity is confined in the cylindrical shell and the (110) [001] and (1 $\bar{1}0$ ) [001] are probably the only slip systems operative. For the closed-end case as shown in Fig. 9, or for thick specimens, the inside cylinder is deformed and other slip systems may be operative to relieve some of the internal stresses created by the local deformation. Both the displacement distributions through the thickness and the delayed bulging effect are indications of the existence of internal stresses.



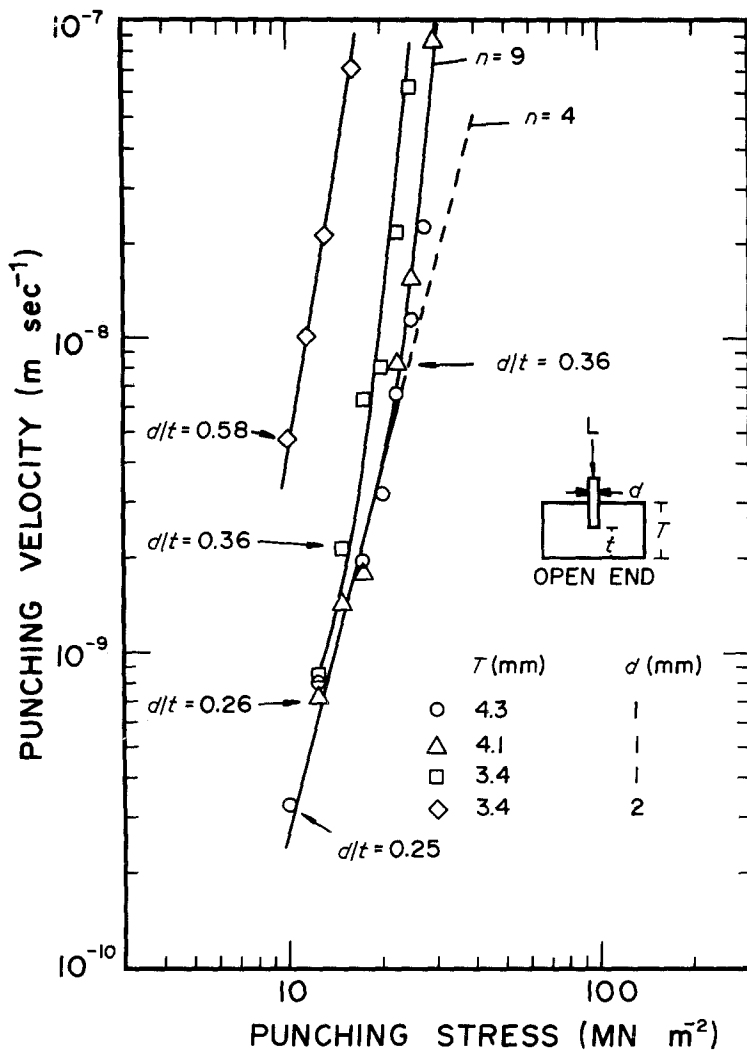


Figure 13 The effect of  $(d/t)$  ratio on the stress dependence of punching velocity.

## 5. Conclusions

(a) Pencil slip was observed in  $\beta$ -tin single crystals by punching in the  $[001]$  direction. A bulge appeared on the opposite surface.

(b) If the opposite surface had a hole in the support to allow free bulging, pencil slip was concentrated in a cylindrical shell whose inner diameter was the same as the punch. The higher the punching stress and/or the larger the punch diameter to crystal thickness ratio,  $(d/t)$ , the thicker was the slip shell. Then the bulge developed into a pyramidal shape with a square base whose sides were parallel to  $[110]$  and  $[1\bar{1}0]$  directions. The bulging velocity was smaller than the punching velocity although they had the same punching-stress dependence.

(c) When the opposite surface was supported

rigidly without a hole, the displacement of the punch only transmitted partially through the thickness. The displacement distribution could be described by a pile-up of circular dislocations. In this case, or in thick crystals so that the  $(d/t)$  ratio was smaller than 0.36, the punching velocity—punching stress relation followed a power law of exponent 4 as in impression creep. For  $(d/t)$  larger than 0.36, the power law exponent increased. When the crystal is not too thick and the impression is not too shallow, delayed bulging appeared after unloading.

## Acknowledgement

This work was supported by Department of Energy through Contract EY-76-S-02-2296\*002.

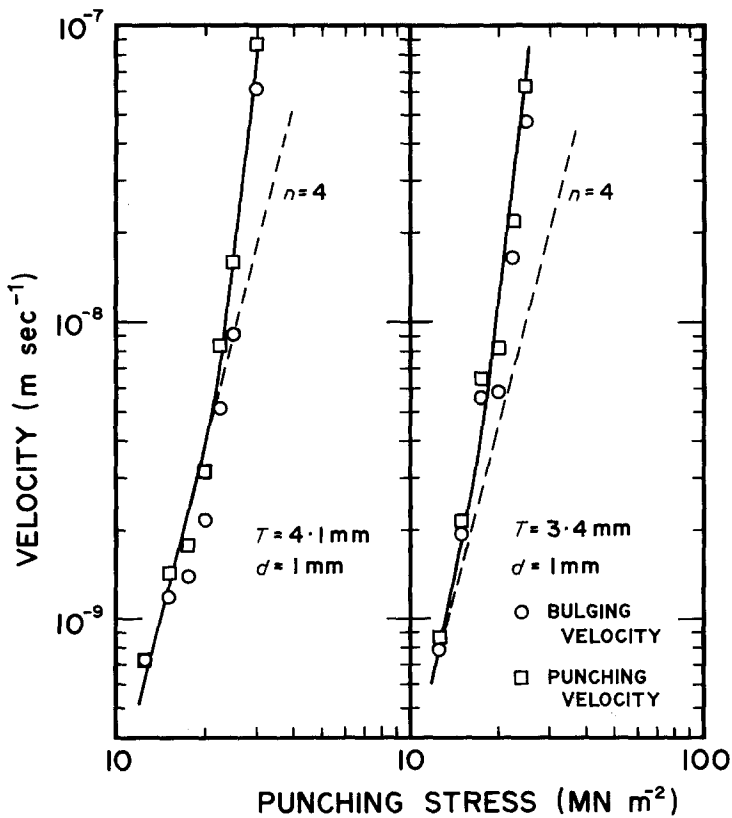


Figure 14 A comparison between punching and bulging velocities.

## References

1. J. TARICCO, *Atti. Accad. Nag. Lincei Re.* 19 (1910) 508.
2. F. R. N. NABARRO, "Theory of Crystal Dislocations" (Clarendon Press, Oxford, 1967) p. 264.
3. O. MÜGGE, *Neues Jb. Miner.* 1 (1914) 43.
4. G. I. TAYLOR and C. F. FLAM, *Proc. Roy. Soc.* A112 (1926) 337.
5. K. M. GREENLAND, *Proc. Roy. Soc.* A163 (1937) 28.
6. J. F. NYE, *ibid.* A198 (1949) 191.
7. A. SMAKULA and M. W. KLEIN, *J. Opt. Soc. Amer.* 39 (1949) 445.
8. F. SEITZ, *Phys. Rev.* 79 (1950) 723.
9. S. N. G. CHU and J. C. M. LI, *Mater. Sci. and Eng.* 39 (1979) 1.
10. G. LEIBFRIED, *Z. Phys.* 130 (1951) 214.
11. A. K. HEAD and N. LOUAT, *Australian J. Phys.* 8 (1955) 1.

Received 20 February and accepted 27 March 1980.